Difference map and its electronic circuit realization

M. García-Martínez · I. Campos-Cantón · E. Campos-Cantón · S. Čelikovský

Abstract This work studies asymptotical dynamical behavior of the one-dimensional discrete-time system, the so-called iterated map. Namely, it introduces a bimodal quadratic map which is obtained as an amplified difference between well-known logistic and tent maps and is denoted as the so-called difference map. Difference map exhibits rich possibilities of the complex dynamical behavior based on its bifurcation parameter selection. The corresponding bifurcations are studied theoretically, numerically and experimentally, presenting numerical simulations and experimental bifurcation diagrams, the stability of this difference map is studied by means of Lyapunov exponent also the difference map is proved to be chaotic according to the Devaney's definition of chaos. Later on, the difference map is implemented as an electronic circuit which is designed and tested. This electronic circuit is built using operational amplifiers, resistors and an analog multiplier. It turns out that this electronic circuit presents fixed points, periodicity, period doubling, chaos and intermittency that match with high accuracy the corresponding theoretically predicted values. Possible applications are shortly discussed, among them possibility of chaos based encryption scheme built in completely independent analog type device.

Keywords chaotic behavior · Lyapunov exponent · bifurcation parameter · bifurcation diagram · stability analysis.

M. García-Martínez.
Division de Matemáticas Aplicadas, Instituto Potosino de Investigación Científica y Tecnológica. Camino a la Presa San José 2055, 78216 México.
Tel.: 01-52-444-8342000.
Fax: 01-52-444-8342010.
E-mail: moises.garcia@ipicyt.edu.mx

I. Campos-Cantón.
Facultad de Ciencias, Universidad Autónoma de San Luis Potosí. Zona universitaria Avenida Salvador Nava S/N, 78290 México.
Tel.: 01-52-444-8262316.
Fax: 01-52-444-8262318.
E-mail: icampos@fciencias.uaslp.mx

E. Campos-Cantón.
Division de Matemáticas Aplicadas, Instituto Potosino de Investigación Científica y Tecnológica. Camino a la Presa San José 2055, 78216 México.
Tel.: 01-52-444-8342000.
Fax: 01-52-444-8342010.
E-mail: eric.campos@ipicyt.edu.mx

S. Čelikovský.
Department of Control Theory, Institute of Information Theory and Automation, Academy of Sciences of the Czech Republic. Pod vodárenskou věží 4, 18208 Prague, CR.
Tel.: 01-42-026-6052020.
Fax: 01-42-028-6890286.
E-mail: celikovs@utia.cas.cz

1 Introduction

Iterated maps are simple looking discrete-time dynamical systems which can exhibit order to chaos transition. It is well-known that only non-monotonous 1-dimensional maps may exhibit complex behaviour, the simplest non-monotonous maps are the so-called unimodal maps. Famous and broadly studied examples of unimodal maps are the tent map and the logistic map, being the subject of constant investigation in many areas such as communication systems [1], generation of pseudorandom sequences [2–4], neural networks [5], switching systems [6] and cryptography [7–11] and part of the interest for these systems is linked to the fact that they provide an easy and pedagogical way to understand how complex and chaotic behavior can arise from simple dynamical models. Even more remarkable is the fact that studies of low-dimensional maps have proven to be fruitful in understanding the basic mechanisms responsible for the appearance of chaos in a large class of dynamical systems.

Further more complex behavior may be provided by the so-called bimodal, or even *k*-modal maps, [12]. This paper introduces yet another bimodal map, constructed based on the difference between logistic and tent map multiplied by a new bifurcation parameter. This new system is therefore called as the **difference** one and is carefully analyzed theoretically, numerically and experimentally through electronic circuit.

One of the most useful and widely accepted definition of chaos is the one by Devaney [13], which we will call Devaney-chaos. Roughly speaking, Devaney chaos consists of three conditions, (1) the sensitive dependence upon the initial condition, (2) the topological transitivity, and (3) the dense distribution of the periodic orbits. The third condition is often omitted for being too stringent [14]. Fortunately, there is another characterization of dynamic behavior, which can be measured by Lyapunov exponents [15–17]. With the aid of their diagnostic, one can measure the average exponential rates of divergence or convergence of nearby orbits in the phase space, overall with their signs, a qualitative picture of the variety of dynamics system's may exhibit, ranging from fixed points via limit cycles and tori to more complex chaotic attractors. Also, bifurcation diagrams are excellent tools to study dynamical behavior and understand mechanisms such as the so-called period-doubling cascades of fixed points, encountered qualitatively in many physical systems of interest or mathematical models that have been electronically implemented [18,19].

Electronic implementation of chaotic systems have been of great help to validate certain theories concerning chaos and have also been applied to several engineering developments. Since its inception three decades ago, there are different implementations of Chua's circuit [20–22]. Historically seen, Chua's circuit was the first successful physical implementation of a system designed to exhibit chaos [23]. This circuit is the first system rigorously proved to be chaotic [24]. Chua's circuit is a continuous time dynamical system where chaos can be observed experimentally. The Chua's diode has been modified to generate multiscroll chaotic which is an extension of Chua type double scroll circuit [25]. The behavior of the difference map is simpler than Chua's circuit to comprehend and it has been proved chaotic. The behavior of Chua's oscillator is due to the fact that it contains five different parameters, whereas for difference map is only one. There are several chaotic circuit which have been reported based on third order differential equation, in the area of continuous time dynamical systems, see [26–30], but few in the area of discrete time dynamical systems furthermore to present advantage and be useful in applications like encryption systems, radar systems, secure communication systems, among others.

Some discrete dynamical systems have been implemented by using digital integrated circuits, for example in [31] presents a digital implementation of the tent map. The problem that arises using digital implementation is that the system only takes a finite number of states. Electronic circuits have been designed, implemented and tested to accurately realize the logistic difference equation [18] or the tent map difference equation [19] by using analog devices in order to have an infinite number of values that can be visited.

In this paper, we enlarge the set of maps known to be chaotic by presenting a chaotic map based on the difference between the logistic map and the tent map. The difference map, more precisely, enables us to construct a bimodal map which is chaotic in the sense that it has positive Lyapunov exponent. We also present one of the simplest electronic implementation of the difference map based on analog devices, which at the same time is a good engineering model of the corresponding mathematical system. Through the variation of only one control parameter, one can examine the bifurcation diagram of the realized system and we have been able to reproduce the theoretical diagram with high accuracy.

The possible application of this circuit implementation would be independent analog chaos generator usable for encryption purposes, e.g. as independent device to cipher. In recent years, a growing number of cryptosystems based on continuous systems utilize the idea of synchronization of chaos. However, recent studies show that the performance of continuous systems is very poor and insecure. The insecurity results mainly from the insensitivity of synchronization to system parameters [32–35] for this reason we used discrete time systems.

This paper is organized as follows. In the next section we recall some basic definitions while section 3 introduces the difference map, including its theoretical and numerical study and presents its properties. Section 4 describes electronic circuit implementation of the difference map, including key complex dynamical behavior that matches the theoretically predicted one. Some conclusions and outlook are given in the final section.

2 Basic definitions

This paper aims to contribute in the area of the one dimensional, discrete time systems and an asymptotic dynamics study, namely to the systems of the form

$$x_{k+1} = f(x_k), \ k = 0, 1, 2, \ldots N.$$

Where $x_k \in \Re$ and x_0 is the initial condition, such a dynamical system is usually referred to as **map**, as it is fully determined by its right hand side. To ensure boundedness of trajectories, the study is usually restricted to maps that are mapping some compact interval into itself and without any loss of generality one may consider the compact interval $[0,1]$ only. The simplest non-monotonous maps are the

so-called unimodal maps, while their generalization, the so-called k-modal maps may present even more rich dynamical behaviors, [12].

To be more specific, denote $\mathscr{I} := [0,1]$ and recall, that the **critical point** c of the continuous piecewise smooth map $f(x) : \mathscr{I} \mapsto \mathscr{I}$ is $c \in \mathscr{I}$ where f is differentiable and $f'(c) = 0$.

Remark 1: The critical point c occurs for $f'(c) = 0$ or $f'(c)$ doesn't exist. But continuous smooth maps always present $f'(c) = 0$.

First, let us repeat the definition of the k-modal map, introduced in [12].

Definition 1 The map $f : \mathscr{I} \mapsto \mathscr{I}$ is called as the k-modal one, if it is continuous on $\mathscr{I}$ and it has k critical points denoted by c_0, $c_1 \ldots c_{k-1}$ in I. Moreover, there exist intervals $\mathscr{I}_i, i = 0, \ldots, k-1, \cup_{i=1}^{k} \mathscr{I}_{i-1} = \mathscr{I}$, such that $\forall i = 0, \ldots, k-1$ it holds $c_i \in \mathscr{I}_i$ and $f(c_i) > f(x,\beta), \forall x \in \mathscr{I}_i$ and $x \neq c_i$, where β is a parameter. The case $k = 1$ will be further simply referred as to the so-called **unimodal** map, while the case $k = 2$ as the **bimodal** one.

Remark 2: The above definition doesn't constraint a function to have only k critical points. However only considered those that are local maximum on a subinterval.

Definition 2 The logistic map is defined as

$$f_L(x,\alpha) = \alpha x(1-x), \tag{1}$$

where parameter $\alpha \in [0,4]$.

The logistic map was first presented by Verhulst [36] as a model for the growth of species and it is one of the classics in the field of discrete nonlinear dynamics. The logistic map has been extensively studied and more properties can be found in [37] while some basic properties can be found in [38,39].

Definition 3 The tent map is defined as

$$f_{T,}(x,\mu) = \begin{cases} \mu x, & \text{for } x < 1/2, \\ \mu(1-x), & \text{for } x \geq 1/2, \end{cases} \tag{2}$$

where parameter $\mu \in [0,2]$.

The logistic and tent maps are obviously unimodal ones, as they are continuous on $\mathscr{I}$ with a single critical point $c_0 = 0.5$ and they increase for $x \in [0,0.5)$ and they decrease for $x \in [0.5,1]$. Their rich complex behavior has been demonstrated many times [40,41], based on the evolution of their bifurcation parameters α, μ.
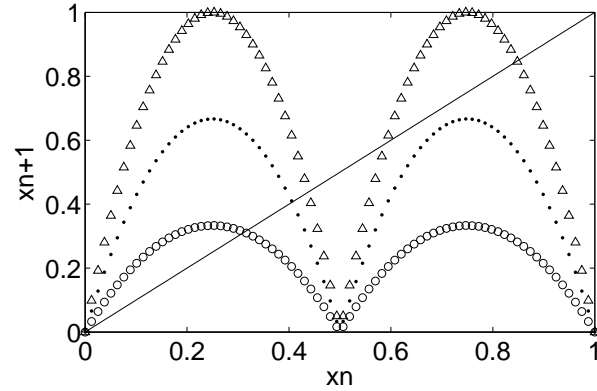

Fig. 1 Difference map for different valued of β: 1.333 (line formed by circles), 2.666 (dotted line) and 4 (line formed by triangles).

Example 1 The following quadratic map

$$f_Q(x,\gamma) = \gamma(1-2x) \begin{cases} x, & \text{if } x < 0.5, \\ (x-1), & \text{other case,} \end{cases} \tag{3}$$

is the bimodal map in the sense of the Definition 1. As a matter of fact, the map given by Eq. (3) has three critical points and two of them are $c_0 = 0.25$ and $c_1 = 0.75$ located at intervals $\mathscr{I}_0 = [0,0.5]$ and $\mathscr{I}_1 = [0.5,1]$, respectively. The other critical point $c = 0.5$ due to $f_Q'(0.5)$ does not exist. Notice that this critical point does not satisfied the definition 1. Thus the map given by Eq. (3) is a bimodal map.

Definition 4 (Devaney's Definition of Chaos)[14]. Let $(X;d)$ be a metric space. Then, a map $f : X \to X$ is said to be **Devaney-chaotic** on X if it satisfies the following conditions.

1. f has **sensitive dependence on initial conditions**. That is, there exists a certain $\varepsilon > 0$ such that, for any $x \in X$ and $\delta > 0$, there exists some $y \in X$ where the distance $d(x;y) < \delta$ and $m \in \aleph = \{1,2,3...\}$ so that the distance $d(f^m(x);f^m(y)) > \varepsilon$.
2. f is **topologically transitive**. That is, for any pair of open sets $U,V \subset X$, there exists a certain $m \in \aleph$ such that $f^m(U) \bigcap V \neq \emptyset$.
3. f has **dense distribution of the periodic orbits**. That is, suppose Y is the set that contains all periodic orbits of f, then for any point $x \in X$, there is a point y in the subset Y arbitrarily close to x.

The concept of neighborhood of a point $x \in X$ is important for demostrating the second condition of Devaney's definition of chaos and is given as follows.

Definition 5 A *neighborhood* of a point $x \in X$ is a set $N_\delta(x)$ consisting of all points $y \in X$ such that the distance $d(x,y) < \delta$. The number δ is called the *radius* of $N_\delta(x)$.
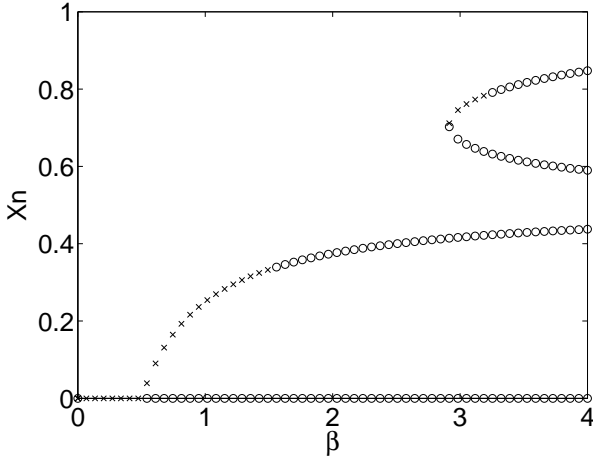
Fig. 2 Stability of the fixed points. The asterisks and circles denote stable and unstable fixed points, respectively.

Fig. 3 Bifurcation diagram for the difference map given by Eq.(4).

3 Difference map

The main contribution of this paper is to present the so-called difference map and to provide its implementation as an electronic circuit. The difference map, denoted as $f_D(x,\beta)$, will be a particular case of the above described bimodal quadratic map Eq.(3) denoted $f_Q(x,\gamma) : [0,1] \to [0,1]$ with $\gamma = 2\beta$, where parameter $\beta \in [0,4]$. This difference map is constructed based on the difference between logistic map and tent map, which explains such a terminology. More precisely, consider the following

Definition 6 Consider the logistic and tent maps with maximum bifurcation parameters $\alpha = 4$, $\mu = 2$. Defined $f_D(x,\beta)$ as the difference between these two maps multiplied by the parameter $\beta \in [0,4]$, namely, $f_D(x,\beta) = \beta(f_L(x,4) - f_T(x,2))$, i.e.:

$$f_D(x,\beta) = \begin{cases} 2\beta x(1-2x), & \text{for } x < \frac{1}{2}; \\ 2\beta(x-1)(1-2x), & \text{for } x \geq \frac{1}{2}. \end{cases} \qquad (4)$$

Indeed, the difference map defined in the Definition 6 is exactly the bimodal map Eq.(3) with $\gamma = 2\beta$. Now, β is a new bifurcation parameter which amplifies the difference between the logistic map and the tent map. This new parameter belongs to the interval $[0,4]$, notice that for $\beta = 4$ the difference map $f_D(x,\beta) : [0,1] \to [0,1]$. Figure 1 shows the difference map given by Eq. (4) for different values of β: 1.333 (line formed by circles), 2.666 (dotted line) and 4 (line formed by triangles). Notice that the difference map always has a fixed point at 0 and it can have others depending the value of β at $\frac{2\beta-1}{4\beta}$, $\frac{6\beta-1-\sqrt{4\beta^2-12\beta+1}}{8\beta}$ and $\frac{6\beta-1+\sqrt{4\beta^2-12\beta+1}}{8\beta}$.

For analyze the asymptotic behavior of the discrete time dynamical system we put the map as its right hand side, i.e. the system
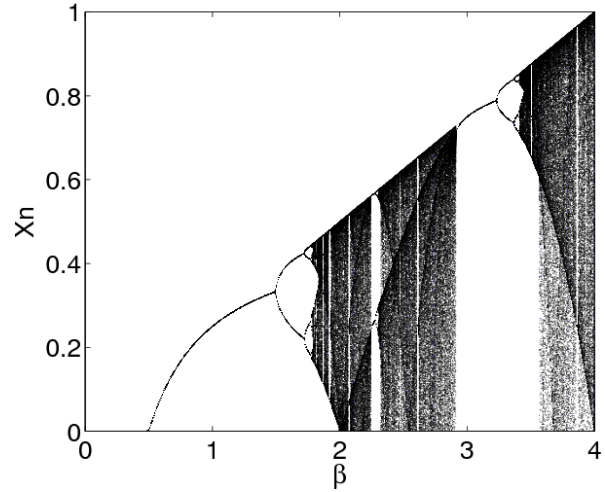
$$x_{k+1} = f_D(x_k,\beta), \text{ for } x_0 \text{ given and } k = 0,1,2,3,\dots$$

The difference map can behave as a bimodal or unimodal map according to the β bifurcation parameter value. For example, if $\beta = 2$, then for any initial condition $x_0 \in [0,1]$, $f_D(x,\beta)$ behaves after the first iteration as an unimodal map $f_D(x,\beta) : [0,0.5] \to [0,0.5]$. The stability of fixed points of the difference map can be attractive or repulsive as is shown in Figure 2. An asterisk denotes an attractive fixed point and a circle denotes a repulsive fixed point. The fixed point located at zero is attractive for $\beta \in [0,0.5]$ and repulsive for $\beta \in [0.5,4]$. The second fixed point is given by $\frac{2\beta-1}{4\beta}$ which is attractive for $\beta \in [0.5,1.495)$ and repulsive for $\beta \in [1.495,4]$. The third fixed point located at $\frac{6\beta-1-\sqrt{4\beta^2-12\beta+1}}{8\beta}$ is always repulsive for $\beta \in [2.915,4]$ and last one given by $\frac{6\beta-1+\sqrt{4\beta^2-12\beta+1}}{8\beta}$ is attractive for $\beta \in [2.915,3.235)$ and repulsive for $\beta \in [3.235,4]$.

It is well known that an attractive fixed point does not let oscillations meanwhile a repulsive fixed point can yield periodic orbits and even chaotic orbits. Figure 3 shows a bifurcation diagram of the orbit of the difference map $\Phi_\beta(x_0)$, which is on $[0,1] \times [0,4]$. Two period doubling bifurcations appear approximately at $\beta = 1.5$ and $\beta = 3.2312$. For $\beta \in [0,2]$ the difference map resembles to the logistic map but it oscillates in the interval $[0,0.5]$, and for $\beta \in [2,4]$ it behaves as a bimodal map and it can oscillate in the interval $[0,1]$.

The Lyapunov exponent, which is denoted by λ, gives the global stability of the system Eq.(3) and it is shown in Figure 4. For $\beta \in [0,0.5]$ the system only has a fixed point which is attractive and $\lambda < 0$, the orbit settles down at the fixed point. For $\beta \in [0.5,1.5)$ the system has two fixed points: one attractive and the other repulsive and $\lambda < 0$ due to the orbit settles down at the attractive fixed point but
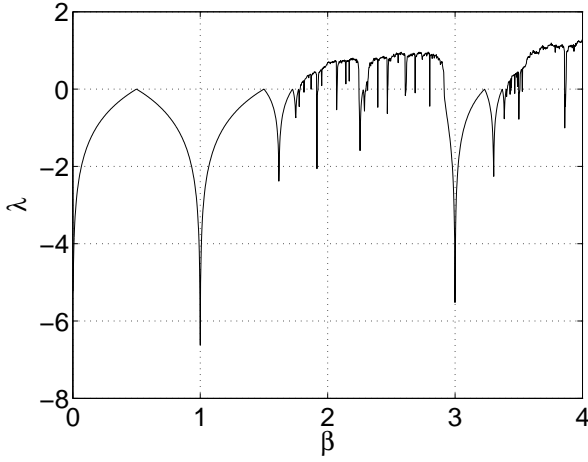
Fig. 4 Lyapunov exponent of the difference map.

Fig. 5 The difference map and the subintervals $J_i^1, i = 0, 1, 2, 3$. Circles denote critical points, squares denote fixed points and triangles denote η.

when $\beta = 1.5$ the systems has a bifurcation and the value of $\lambda = 0$. For $\beta \in (1.5, 2.915)$ the system has two fixed points and both are repulsive and $\lambda < 0$ when the orbit periodically oscillates or $\lambda > 0$ when the orbit oscillates chaotically. For $\beta \in (2.915, 3.235)$ the system has four fixed points and three of them are repulsive and the other fixed point is attractive, $\lambda < 0$, thus the orbit settles down at the attractive fixed point again and also when $\beta = 3.235$ another bifurcation occurs and therefore $\lambda = 0$. For $\beta \in (3.235, 4]$ the system maintains its four fixed points but now all of them are repulsive. The orbit oscillates periodically or chaotically when $\lambda < 0$ and $\lambda > 0$, respectively.

Theorem 1 *The difference map $f_D(x, \beta)$ is Devaney-chaotic on $[0, 1]$ for $\beta = 4$.*

Proof From Definition 4, we need to prove three conditions, (1) the sensitive dependence upon the initial condition, (2) the topological transitivity and (3) the dense distribution of the periodic orbits.

We start by demonstrating the last property. We need to prove that there exists a Y subset of the interval $I = [0, 1]$ constitutes for periodic orbits, and that Y is dense in I. The I interval can be divided by $J_0^1 = [0, c_0^1], J_1^1 = [c_0^1, \eta_0^0 = 0.5]$, $J_2^1 = [\eta_0^0 = 0.5, c_1^1]$ and $J_3^1 = [c_1^1, 1]$, (see Figure 5) each intervals contains one fixed point of the difference map f_D, $\Delta^1 = \{p_0^1 = 0, p_1^1 = 0.4375, p_2^1 = 0.5899, p_3^1 = 0.8476\}$, respectively. These fixed points in the closed interval I belong to Y as periodic orbits of period one, where $c_0^1 = 0.25$ and $c_1^1 = 0.75$ are the critical points. Notice that $f_D : J_i^1 \rightarrow [0, 1]$, $i = 0, \dots, 3$, then each subinterval resembles the difference map for f_D^2. Notice that $f_D(0) = f_D(0.5) = f_D(1) = 0$ and $f_D(c_0^1 = 0.25) = f_D(c_1^1 = 0.75) = 1$. The foregoing observation let us to infer that for all $x \in I$ and if $f_D^k(x) = 0.5$ then
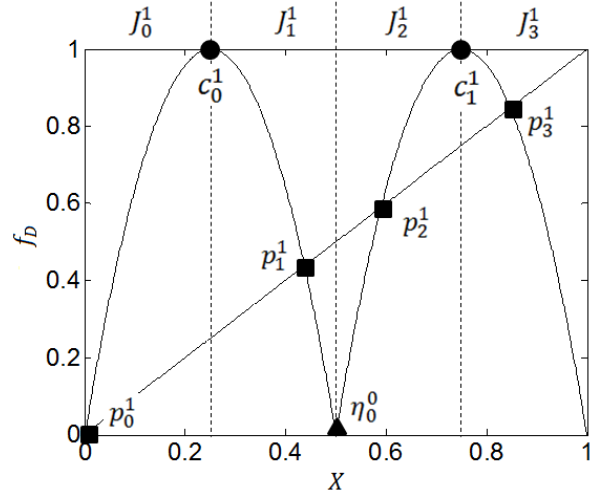
$$f_D^{k+1}(x) = 0.$$

The fixed points correspond to the intersection between f_D and the identity function $f_I(x) = x$. If we consider the intersection between the second iteration f_D^2 and f_I we find that these functions intersect at 16 points, the set of fixed points Δ^1 and a set of periodic points of period two Δ^2. Now the interval I consisted of 16 subintervals $J_0^2 = [0, c_0^2]$, $J_1^2 = [c_0^2, \eta_0^1], J_2^2 = [\eta_0^1, c_1^2], J_3^2 = [c_1^2, c_0^1], J_4^2 = [c_0^1, c_2^2], J_5^2 = [c_2^2, \eta_1^1], J_6^2 = [\eta_1^1, c_3^2], J_7^2 = [c_3^2, 0.5], J_8^2 = [0.5, c_4^2], \quad J_9^2 = [c_4^2, \eta_2^1], J_{10}^2 = [\eta_2^1, c_5^2], J_{11}^2 = [c_5^2, c_1^1], J_{12}^2 = [c_1^1, c_6^2], J_{13}^2 = [c_6^2, \eta_3^1], J_{14}^2 = [\eta_3^1, c_7^2]$ and $J_{15}^2 = [c_7^2, 1]$. Figure 6 shows the subintervals $J_i^2, i = 0, 1, 2, \dots, 15$, the fixed points are marked with squares and the periodic points with period two with asterisk, $\Delta^2 = p_0^2, p_1^2, p_2^2, p_3^2, \dots, p_{11}^2$. The set $\{c_0^2, c_1^2, c_2^2, c_3^2, c_4^2, c_5^2, c_6^2, c_7^2\}$ contains the critical points of f_D^2 and $\eta_i^1 = f_D(x) = 0.5, i = 0, \dots, 3$. The periodic points of period one and two belong to $Y \supset \Delta^1 \cup \Delta^2$. In general, the intersections between f_D^n and f_I give the periodic points of period n and may be periodic points of less period. I is comprised by subintervals $J_i^n, i = 0, \dots, 4^n - 1$ and the end points of the intervals are given by the critical points of $f_D^k, \eta^{k-1} = f_D^{k-1}(x) = 0.5$, $k = 1, \dots, n$, and the previous end points. The particularity is that each subinterval J_i^n contains at least a periodic point and $|J_i^n| \rightarrow 0$ when n $\rightarrow \infty$. Thus for any $x \in I$, there is a point y in the subset Y arbitrarily close to x, so this proves that periodic points are dense in $[0, 1]$.

In order to demonstrate that f_D is **topologically transitive**. We consider a pair of open sets $N_\delta(y_1), N_\delta(y_2) \subset I$, for any $y_1, y_2 \in I$, we need to show that there exists a certain $m \in N = \{1, 2, 3, \dots\}$ such that $f_D^m(N_\delta(y_1)) \cap N_\delta(y_2) \neq \emptyset$, i. e. , we need to show that at least one orbit with initial condition $x_0 \in N_\delta(y_1)$ evolves to $N_\delta(y_2) \ni f_D^m(x_0)$. First we consider two open sets $N_\delta(y_1)$ and $N_\delta(y_2)$ arbitrarily located at
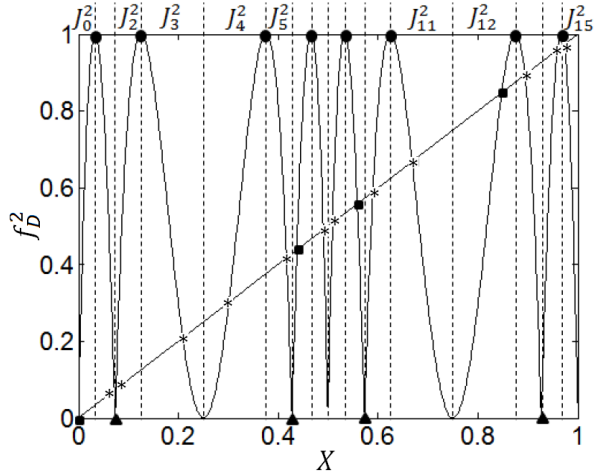
Fig. 6 Distribution of the periodic orbits of period two, circles denote critical points, squares denote fixed points, and triangles denote η.
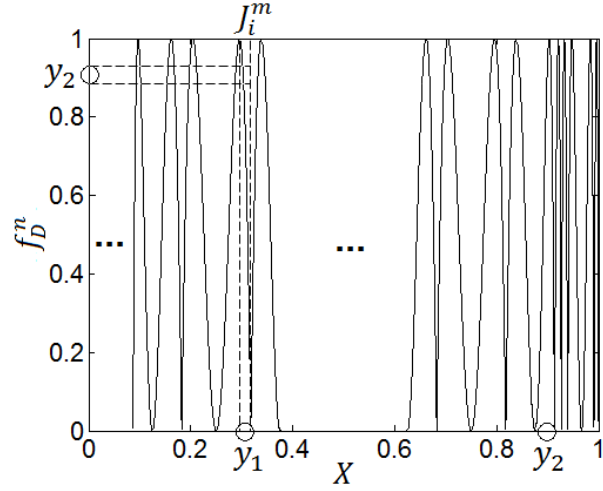

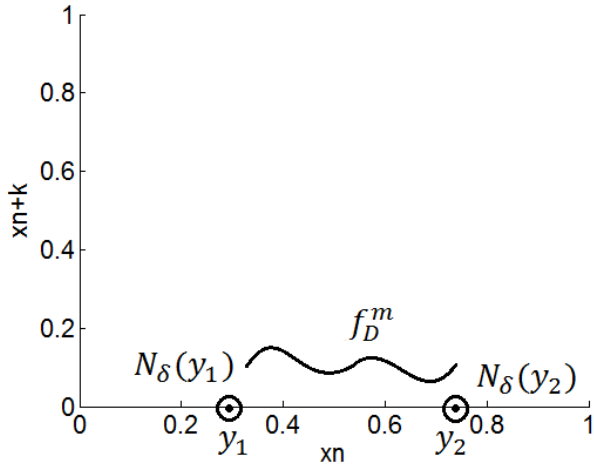**Fig. 8** Transitivity of an orbit of period n (f_D^n) of difference map.

Fig. 7 There exists an orbit such two points with a neighborhood comes arbitrarily close.

Fig. 9 A zoom of figure 8 in order to appreciate the transitivity of an orbit of period n where $f(J_i^m) \supseteq I \supset N_\delta(y_1)$.

I as is shown in Figure 7. In the previous paragraphs we discuss that each subintervals J_i^k tends to zero when k tends to infinity, also we know that each subinterval J_i^k is mapped onto the interval I, $f_D^k : J_i^k \to I$. Thus, consider a subinterval $J_i^m \subset N_\delta(y_1)$. as is shown in Figures 8 and 9. Accordingly $f(J_i^m) = I \supset N_\delta(y_2)$ then $f_D^m(x_0) \in N_\delta(y_2)$, for any $x_0 \in N_\delta(y_1)$, this proves that f_D is topologically transitive.

Finally, we need to demonstrate **sensitive dependence on initial conditions** of the difference map, so that we start to define $\varepsilon = |I|/2$, where $|I| = 1$, such that for any $x_{01} \in I$ and any $\delta > 0$ there is a $x_{02} \in N_\delta(x_{01})$ such that the distance between $|f_D^m(x_{01}) - f_D^m(x_{02})| \geq \varepsilon$.

Remak 3: The definition of sensitivity does not require that the orbit of x_{02} remain far from x_{01} for all iterations. We only need one point on the orbit to be far from the corresponding iterate of x_{01}.
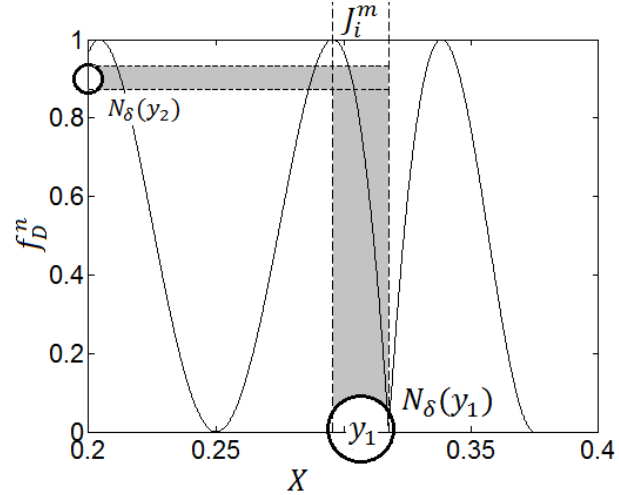
So if we consider the subinterval J_i^{m-1} such that $J_i^{m-1} \subset N_\delta(x_{01})$ then there is a $x_{02} \in J_i^{m-1}$ such that $|f_D^m(x_{01}) - f_D^m(x_{02})| \geq 1/2$. Thus we have sensitive dependence on initial conditions. Now the proof is completed.

4 Electronic implementation of the difference map

Devaney's definition of chaos makes sense only for the iterative dynamical systems on continua. From Definition 4, one can immediately see that no map is Devaney-chaotic if X is a discrete space. This is a strong condition why chaotic discrete dynamical systems need to be implemented electronically by analog devices in both of its parts: 1) the electronic implementation of the map and 2) the electronic implementation of the iterative process, see Fig. 10. First we will focus on explaining the circuit of the difference map.
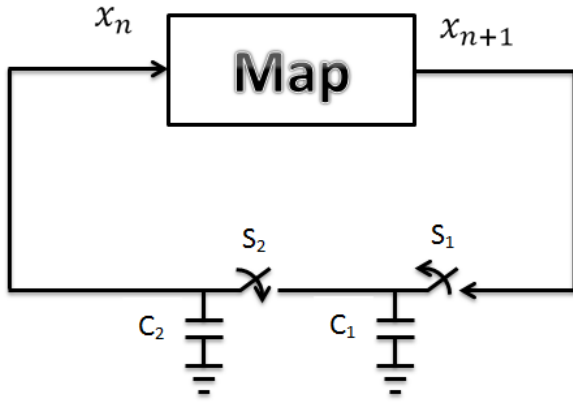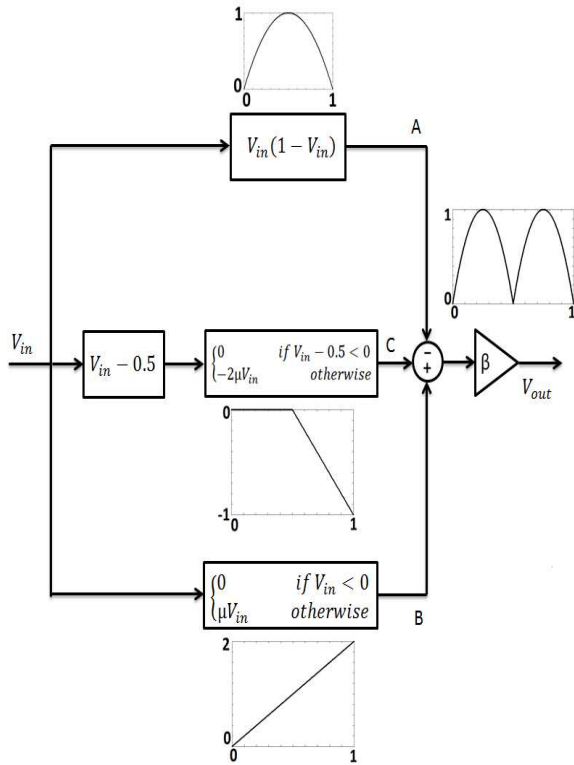
Fig. 10 Circuit diagram of an electronic map.

Fig. 11 Block diagram of the difference map used to construct the electronic circuit.

Fig. 12 Schematic diagram of the difference map electronic circuit.

The experimental development of this map is achieved by means of electronic devices as multipliers, operational amplifiers, diodes and resistors. In the same spirit that other implementations of this kind of circuits [18,42] analog multipliers have been employed with a normalization of the signal by a factor of about 10. This normalization is necessary because of the physical restrictions in the analog multiplier. The starting point is a block diagram of the difference map that is shown in Figure 11. The output of the electronic circuit has three branches: The former generates the logistic map (node A) and the last two correspond to the tent map (node B and C). Typically, these circuits contain several op-
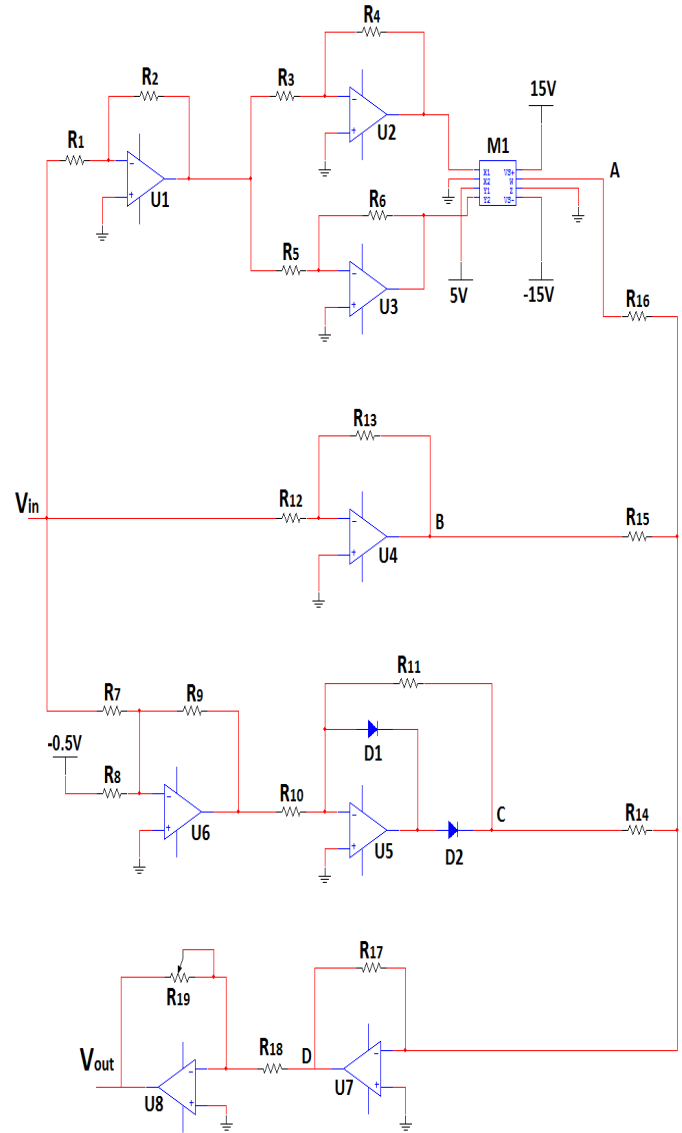
erational amplifiers, which perform linear operations (e.g., integration and summation), as well as a couple of integrated circuits that perform the nonlinear operations (i.e., multiplication). Here, we describe a new circuit that contains active components, speeds of radio frequencies, and is capable of reproducing the transition from steady state to chaos as observed in the difference map equation when the bifurcation parameter is varied.

Figure 12 shows a schematic diagram of the electronic circuit realization of the difference map. The output of the circuit is analyzed using the voltages at the nodes: A, B, C, D.

The A node voltage is given by the $M1$ multiplier which has four input terminals (x_1, x_2, y_1, y_2) and an output terminal given by $W = \frac{(x_1 - x_2)(y_1 - y_2)}{10}$. Inputs $x_1 = V_{in}(R_2 R_4)/(R_1 R_3)$

Table 1 The values of the electronic components employed in the construction of the difference map electronic circuit.

Device	Value
$R_1, R_3, R_5, R_6, R_7, R_8, R_9,$	
$R_{10}, R_{12}, R_{16}, R_{18}$	10kΩ Resistor
R_4	4kΩ Resistor
$R_{11}, R_{14}, R_{15}, R_{17}$	40kΩ Resistor
R_{13}	20kΩ Resistor
R_{19}	40kΩ Potentiometer
D1,D2	1N4148 Diode
U1,U2,U3,U4,U5,U6,U7,U8	TL084 Op. Amp.
M1	AD633 Multiplier

and $y_2 = V_{in}(R_2 R_6)/(R_1 R_5)$ are given by operational amplifiers U2 and U3, respectively. Inputs x_2 and y_1 are 0V and 5V, respectively. Hence, the output at A node is given by

$$V_A = \left(V_{in} \frac{R_2 R_4}{R_1 R_3} \right) \left(5 - V_{in} \frac{R_2 R_6}{R_1 R_5} \right) / 10, \qquad (5)$$

the A node voltage is $V_{in}(1 - V_{in})$ after evaluating components values of the Table 1, this signal corresponds to the logistic map f_L without considering the α bifurcation parameter .

The B node voltage is given by the U4 amplifier output which is fed back to the inverting input, the output voltage is

$$V_B = -V_{in} R_{13}/R_{12}. \qquad (6)$$

The C node voltage is given by the U5 amplifier output which is a piecewise linear signal, then

$$V_C = \begin{cases} 0, & \text{for } V_{in} < \dfrac{R_7}{2R_8}; \\ \dfrac{R_{11}}{R_{10}} \left(\dfrac{R_9 V_{in}}{R_7} - \dfrac{R_9}{2R_8} \right), & \text{for } V_{in} \geq \dfrac{R_7}{2R_8}. \end{cases} \qquad (7)$$

Equations 6 and 7 correspond to the tent map, remember that $f_T(x, \mu)$ is defined in two parts, to ensure that the map is symmetric the bifurcation parameter μ must be equal on both sides. We can see that μ is given by R_{13}/R_{12} and $R_{11}/(2R_{10})$. This yields the following restrictions $R_{11} = 2R_{13}$ and $R_{10} = R_{12}$.

The U7 amplifier output is the adding of A, B and C node voltages which corresponds to D node voltage, giving

$$V_D = -R_{17} \left(\frac{V_A}{R_{16}} + \frac{V_B}{R_{15}} + \frac{V_C}{R_{14}} \right), \qquad (8)$$

it is worth mentioning that the ration R_{17}/R_{16} is the parameter $\alpha = 4$. Thus, the D node voltage is $(-f_L + f_T)$ that is indeed the difference map invested without taking account of the bifurcation parameter β.

Finally, the V_{out} voltage is given by the U8 inverting amplifier, the output is $(R_{19}/R_{18})V_D$. Assuming ideal perfor-
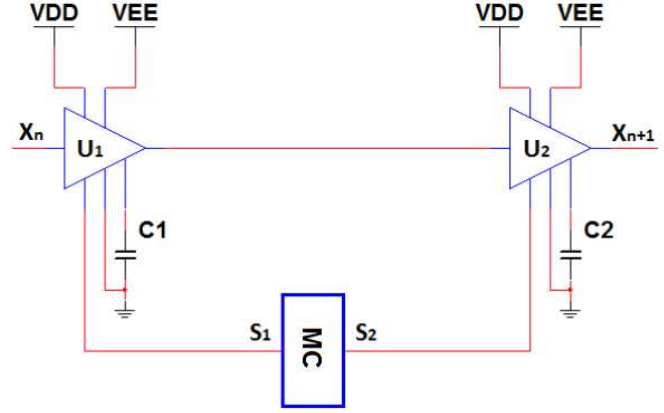

Fig. 13 Schematic diagram of the iterative circuit, U1 and U2 are LF398 and the MC microcontroller is a PIC16F88.

mance from all components, the circuit output in Fig. 12 is modeled by the following equation:

$$V_{out} = \frac{R_{19}}{R_{18}} \begin{cases} 4V_{in}(1 - V_{in}) - 2V_{in}, & \text{for } V_{in} < \frac{1}{2}\text{V}; \\ 4V_{in}(1 - V_{in}) + 2V_{in} - 2, & \text{for } V_{in} \geq \frac{1}{2}\text{V}. \end{cases} \qquad (9)$$

Then, equation 4 can be derived from equation 9 by the change of variables $V_{in} = x_n$, $V_{out} = x_{n+1}$ and $\beta = R_{19}/R_{18}$.

The second part of the circuit is responsible to make the iterative operation, (see Fig. 10), this circuit considers a microcontroller PIC16F88 of Microchip, and two hold and sample LF398 of National Semiconductors in order to hold the V_{out} signal given by Eq. 9. That is, the hold and sample circuits have been used as an analog memory in order to store the value of x_k and get x_{k+1}, thus this is the way how the electronic circuit shown in Fig. 12 generates the iterative operation. Obviously, there are different ways to perform this iterative operation, but this is a matter that depends of the designer and the application. Figure 13 shows a schematic diagram for this part of the circuit, one can see that each device LF398 (U1 and U2) has an input for activation, the signal for both hold and sample comes from the microcontroller PIC16F88.

The time of each trigger to activate the devices is defined for the designer, in this case we set 20 ms between each shot, where the duration of each shot is 1 ms, these times are programmed into the microcontroller and can vary depending the application. Figure 14 shows a diagram with the time of activation of each hold and sample.

Once both circuits are tuned in correct operation the difference map begins its iterative process. Figure 15 shows a time series for $\beta = 4$. Despite of parasitic reactance, finite bandwidth of active components, and other experimental perturbations, the presented electronic circuit displays closely the behavior of the mathematical model given by Eq. 4. We have implemented this design on a printed circuit board (PCB) manufactured in our laboratory. In the experimental circuit the TL084 operational amplifiers and LF398
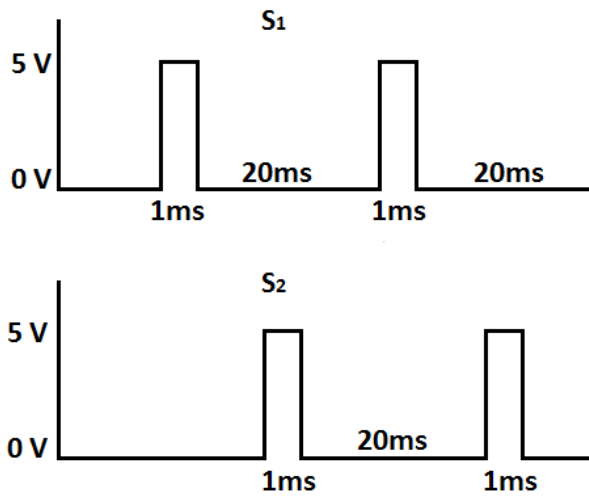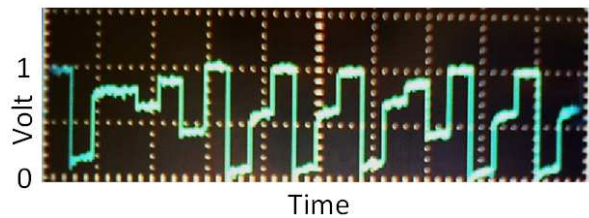
Fig. 14 Times of activation for hold and sample.

Fig. 15 The time series with chaotic dynamics generated by the tent map for $\beta = 4$.
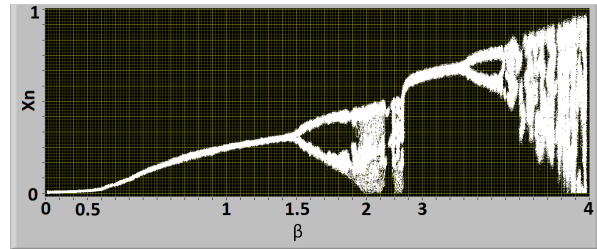

Fig. 16 Experimental bifurcation diagram for the difference map.

behavior in means of Lyapunov exponent also one of the main properties of this map is that it has two critical points making this a bimodal map but setting the β parameter it can show the behavior of unimodal map or a bimodal map, besides this paper includes a theoretical analysis of their equilibrium points as well as the stability also were obtained the corresponding bifurcation diagram from numerical simulations and finally a simple difference map electronic circuit has been presented here and its implementation using analog components as multipliers, operational amplifiers, diodes, and resistors was also provided. Therefore, it can be assembled even by students at the level of an undergraduate laboratory. Its experimental behavior was tested and compared with the numerical behavior given by the difference map Eq. 4. The circuit replicates the whole known range of behaviors of the difference map and the it have many potential applications, for example: random number generation, frequency hopping, ranging, and spread-spectrum communications. As the outlook for further research, the possibility of encryption using stream ciphers based on the analog circuit independent from computer with date to be encrypted is considered. This is the object of currently ongoing research.

hold and sample have been supplied with a power source at $\pm 15\text{V}$ and soldered directly to the PCB without a socket, also a source power of -0.5V is used for proper operation of the tent map. The voltage Vdc has been supplied by a variable dc supply with an output range of $0 - 15\text{V}$.

The value of the bifurcation parameter β can be fixed at certain values by simply adjusting the potentiometer R_{19} located in the operational amplifiers U8. In order to explore the full range of the dynamics accessible to this circuit, we have experimented with different values for R_{19}. The value of this potentiometer has been adjusted in the closed interval $[0\ \Omega, 40\ \text{k}\Omega]$. Then the value of β has been varied to obtain the bifurcation diagram shown in Fig. 16, where fixed points, periodic oscillations, period-doubling cascade and chaos can be clearly seen and it can be seen that the circuit exhibits the entire range of behaviors of the difference map. In fact, our experimental results of the dynamics of this circuit are found to be in good agreement with numerical simulations.

5 Conclusion

In this paper we introduced a new discrete-time dynamical system of 1-dimension that works in a closed interval and is based on the logistic and tent map which presents chaotic

References

1. A.D. Mengue, B. Z. Essimbi C.: Secure communication using chaotic synchronization in mutually coupled semiconductor lasers, Nonlinear Dyn, **70**(2), 1241-1253, (2012).
2. Xing-yuanWang, Xue Qin Mieczyslaw Jessa: A new pseudo-random number generator based on CML and chaotic iteration, Nonlinear Dyn **70**, 15891592, (2012).
3. Vinod Patidar, K. K. Sud, N. K. Pareel: A Pseudo Random Bit Generator Based on Chaotic Logistic Map and its Statistical Testing, Informatica **33**, 441-452, (2009)
4. Xing-Yuan, Yi-Xin Xie: A Desing Of Pseudo-Random Bit Generator Based on Single Chaotic System, International Journal of Modern Physics C, **23**(3), 1250024, (2012).

5. An-Min Zou, Krishna Dev Kumar, Ramin Pashaie, Nabil H. Farhat: Neural network-based adaptive output feedback formation control for multi-agent systems, Nonlinear Dyn, **70**, 12831296, (2012).

6. Yonggang Chen, Shumin Fei, Kanjian Zhang: Stabilization of impulsive switched linear systems with saturated control input, Nonlinear Dyn, **69**, 793804, (2012).

7. Sahar Mazloom, Amir Masud Eftekhari- Moghadam: Color image encryption based on Coupled Nonlinear Chaotic Map, Chaos, Solitons and Fractals, **.42**, 1745-1754, (2009).

8. I. Shatheesh Sam, P. Devaraj, R.S. Bhuvaneswaran: An intertwining chaotic maps based image encryption scheme, Nonlinear Dyn **69**, 19952007, (2012).

9. Seyyed Mohammad Reza Farschi, H. Farschi: A novel chaotic approach for information hiding in image, Nonlinear Dyn, **69**, 15251539, (2012).

10. Iqtadar Hussain, Tariq Shah, Muhammad Asif Gondal: Image encryption algorithm based on PGL(2,GF(2^8)) S-boxes and TD-ERCS chaotic sequence, Nonlinear Dyn, **70**, 181187, (2012).

11. H.S. Kwok, Wallace K.S. Tang: A fast image encryption system based on chaotic maps with finite precision representation, Chaos, Solitons and Fractals, **32**, 1518-1529, (2007).

12. E. Campos-Cantón, R. Femat and A.N. Pisarchik: A family of multimodal dynamic maps, Commun. Nonlinear Sci. Numer. Simulat., **9**, 3457-3462, (2011).

13. R. Devaney, An Introduction to Chaotic Dynamical Systems, Westview Press, 2nd ed., (2003).

14. B. Kahng: Redefining Chaos: Devaney-chaos for Piecewise Continuous Dynamical Systems, International Journal of Mathematical Models and Methods in Applied Scientifics, **3**(4), 317-326, (2009).

15. Changpin Li and Guanrong Chen: Estimating the Lyapunov exponents of discrete systems, Chaos, **14**, 343-346, (2004).

16. M. Sano, Y. Sawada: Measurement of the Lyapunov Spectrum from a Chaotic Time Series, Physical Review Letters, **55**, 1082-1085, (1985).

17. Caixia Yang, Christine QiongWu, Pei Zhang: Estimation of Lyapunov exponents from a time series for n-dimensional state space using nonlinear mapping, Nonlinear Dyn **69**, 14931507, (2012).

18. M. Suneel: Electronic circuit realization of the logistic map, Sadhana, **31**, 69-78, (2006).

19. I. Campos-Cantón, E. Campos-Cantón, J. S. Murguía, H. C. Rosu. A simple electronic circuit realization of the tent map, Chaos, Solitons and Fractals, **1**, 12-16, (2009).

20. R. Senani and S. Gupta: Implementation of Chua's chaotic circuit using current feedback op-amps, Electronics Letters, **34**(9), 829-830, (1998).

21. Tanmoy Banerjee: Single amplifier biquad based inductor-free Chuas circuit, Nonlinear Dyn, **68**, 565573, (2012).

22. G. Gandhi: An Improved Chua's Circuit and Its Use in Hyperchaotic Circuit, Analog Integrated Circuits and Signal Processing, **46**(2), 173-178, (2006).

23. T. Matsumoto: A chaotic attractor from Chua's circuit, IEEE Trans. Circuits Syst I, **31**(12), 1055-1058, (1984).

24. L. Chua, M. Komuro, and T. Matsumoto: The double scroll family: Parts I and II, IEEE Trans. Circuits and Syst I, **33**, 1073-1118, (1986).

25. A. Radwan, A. Soliman, and A. El-Sedeek: MOS realization of the double-scroll-like chaotic equation, IEEE Trans. Circuits and Systems I, **50**(2), 285-288, (2003).

26. M. Yalcin, J. Suykens, J. Vandewalle, and S. Ozoguz: Families of scroll grid attractors, International Journal of Bifurcation and Chaos, **12**(1), 23-41, (2002).

27. R. Kilic: On Current Feedback Operational Amplifier-Based Realization of Chua's Circuit, Circuits, Systems and Signal Processing, **22**(5), 475-491, (2003).

28. R. Kilic: Experimental Study of CFOA-Based Inductorless Chua's Circuit, International Journal of Bifurcation and Chaos, **14**, 1369-1374, (2004).

29. K. O'Donoghue, P. Forbes, and M. Kennedy: A Fast And Simple Implementation of Chua's Oscillator With Cubic-Like Nonliearity, International Journal of Bifurcation and Chaos, **15**, 2959-2972, (2005).

30. J. L*ü* and G. Chen: Generating multiscroll chaotic attractors: Theories, methods and applications, International Journal of Bifurcation and Chaos, **16**(4), 775-858, (2006).

31. T. Addabbo, M. Alioto, A. Fort, S. Rocchi and V. Vignoli: The digital tent map: performace analysis and optimized design as a low-complexity source of pseudorandom bits, IEEE Transaction on Instrumentation and measurement, **55**(5), 1451-1458, (2006).

32. Perez G, Cerdeira H.: Extracting messages masked by chaos, Phys Rev Lett, **74**, 1970-1973, (1995).

33. Short KM, Parker AT.: Unmasking a hyperchaotic communication scheme, Phys Rev E, **58**, 1159-62, (1998).

34. Zhou C, Lai CH.: Extracting messages masked by chaotic signals of time-elay systems, Phys Rev E, **60**, 320-323, (1999).

35. Yu Zhang, Chengqing Li, Qin Li, Dan Zhang, Shi Shu: Breaking a chaotic image encryption algorithm based on perceptron model, Nonlinear Dyn 69, 10911096, (2012).

36. P.F. Verhulst: Notice sur la loi que la population poursuit dans son accroissement, Correspondance mathématique et physique, **10**, 113-121, (1838).

37. R.A. Holmgren: A First Course in Discrete Dynamical Systems, New York: Springer-Verlag, (1996).

38. S. Lynch: Dynamical Systems With Applications, Birkhauser/Springer, Boston (2010).

39. Chai Wah Wu, Nikolai F. Rul'kov: Studying Chaos via 1-D Maps-A Tutorial, IEEE Trans. Circuits Syst. I, **40**, 707-721, (1993).

40. Li C.: A new method of determining chaos-parameter-region for the tent map, Chaos, Solitons and Fractals, **21**, 863-867, (2004).

41. Huang W.: On complete chaotic maps with tent-maps-like structures, Chaos, Solitons and Fractals, **24**, 287-299, (2005).

42. JN. Blakely, MB. Eskridge and NJ. Corron: A simple Lorenz circuit and its radio frequency implementation, Chaos, **17**, 023112-023112-5, (2007).